

UNCLASSIFIED

SECURITY CLASSIFICATION OF THIS PAGE

DTIC FILE COPY

②

REPORT DOCUMENTATION PAGE

Form Approved
OMB No. 0704-0188

1b. RESTRICTIVE MARKINGS	
3. DISTRIBUTION/AVAILABILITY OF REPORT Approved for public release; distribution unlimited	
4. PERFORMING ORGANIZATION REPORT NUMBER(S) UBUFALLO/DC/90/TR-31	
5. MONITORING ORGANIZATION REPORT NUMBER(S)	
6a. NAME OF PERFORMING ORGANIZATION Depts. Chemistry & Physics State University of New York	6b. OFFICE SYMBOL (If applicable)
7a. NAME OF MONITORING ORGANIZATION	
6c. ADDRESS (City, State, and ZIP Code) Fronczak Hall, Amherst Campus Buffalo, New York 14260	7b. ADDRESS (City, State, and ZIP Code) Chemistry Program 800 N. Quincy Street Arlington, Virginia 22217
8a. NAME OF FUNDING/SPONSORING ORGANIZATION Office of Naval Research	8b. OFFICE SYMBOL (If applicable)
9. PROCUREMENT INSTRUMENT IDENTIFICATION NUMBER Grant N00014-90-J-1193	
8c. ADDRESS (City, State, and ZIP Code) Chemistry Program 800 N. Quincy Street Arlington, Virginia 22217	10. SOURCE OF FUNDING NUMBERS
	PROGRAM ELEMENT NO.
	PROJECT NO.
	TASK NO.
	WORK UNIT ACCESSION NO.
11. TITLE (Include Security Classification) Position Expectation Value and Oscillator Strength of a Biased Asymmetric Quantum Well	
12. PERSONAL AUTHOR(S) Lakshmi N. Pandey and Thomas F. George	
13a. TYPE OF REPORT	13b. TIME COVERED FROM _____ TO _____
	14. DATE OF REPORT (Year, Month, Day) December 1990
15. PAGE COUNT 22	
16. SUPPLEMENTARY NOTATION Prepared for publication in <i>Superlattices and Microstructures</i>	
17. COSATI CODES	
FIELD	GROUP
	SUB-GROUP
18. SUBJECT TERMS (Continue on reverse if necessary and identify by block number)	
QUANTUM WELL /	
BIASED ASYMMETRIC /	
OSCILLATOR STRENGTH.	
19. ABSTRACT (Continue on reverse if necessary and identify by block number)	
<p>The change in the position expectation values of an electron in the first three quasibound states of the structure as a function of the external (biased) voltage is calculated. At the resonance voltage, the most probable position to find an electron in the second and third quasibound states lies in the barrier separating the two wells, and these two states interchange their identities, meaning that the ground state of the narrow well becomes the first-excited state of the wide well and vice versa. (Keywords)</p>	
20. DISTRIBUTION/AVAILABILITY OF ABSTRACT <input checked="" type="checkbox"/> UNCLASSIFIED/UNLIMITED <input checked="" type="checkbox"/> SAME AS RPT <input type="checkbox"/> DTIC USERS	
21. ABSTRACT SECURITY CLASSIFICATION Unclassified	
22a. NAME OF RESPONSIBLE INDIVIDUAL Dr. David L. Nelson	22b. TELEPHONE (Include Area Code) (202) 696-4410
22c. OFFICE SYMBOL	

DTIC
ELECTE
DEC 10 1990
S E D

OFFICE OF NAVAL RESEARCH

Grant N00014-90-J-1193

TECHNICAL REPORT No. 31

Position Expectation Value and Oscillator Strength of a Biased Asymmetric Quantum Well

by

Lakshmi N. Pandey and Thomas F. George

Prepared for publication

in

Superlattices and Microstructures

Departments of Chemistry and Physics
State University of New York at Buffalo
Buffalo, New York 14260

December 1990

Reproduction in whole or in part is permitted for any purpose of the
United States Government.

This document has been approved for public release and sale;
its distribution is unlimited.

POSITON EXPECTATION VALUE AND OSCILLATOR STRENGTH OF A BIASED ASYMMETRIC QUANTUM WELL

Lakshmi N. Pandey and Thomas F. George
Departments of Physics & Astronomy and Chemistry
Center for Electronic and Electro-optic Materials
State University of New York at Buffalo
Buffalo, New York 14260

(Received 10 October 1990)

An asymmetric quantum well consisting of one narrow and one wide well separated by a thick barrier is investigated. We calculate the change in the position expectation values of an electron in the first three quasibound states of the structure as a biased voltage increases. The value in the first quasibound state, which is the ground state of the wide well, shifts toward the right wall of the well. It has been found earlier that for a certain applied voltage, the first and second states of this whole structure, which are actually the ground state of the narrow well and the first-excited state of the wide well, respectively, coincide to give rise to resonant tunneling. At this resonance voltage, we see that the most probable position to find an electron in the second and third quasibound states lies in the barrier separating the two wells. Furthermore, these two states interchange their identities, meaning that the ground state of the narrow well becomes the first-excited state of the wide well and vice versa. We also calculate the oscillator strengths for transitions from the ground state of the wide well to the ground state of the narrow well and the first-excited state of wide well, and from the ground state of the narrow well to the first-excited state of the wide well. A similar conclusion can be drawn regarding the interchange of identities between the second and third quasibound states of the structure from the changes in oscillator strengths as a function of applied voltage. The oscillator strength for the transition from the ground state of the narrow well to the first-excited state of the wide well peaks at the resonant voltage.

or

on

on/

Availability Codes

Dist	Avail and/or Special	
A-1		

90 12 : 7" 070

1. Introduction

The physics of a one-dimensional quantum well has been the subject of experimental and theoretical investigations since the pioneering study of Esaki and Tsu¹ in order to understand some of the properties of heterostructure semiconductors. Modern technological advances, such as molecular beam epitaxy, have made it possible to fabricate quantum wells of specific height and width. Recently, a quantum well structure consisting of two wells of different thicknesses separated by a barrier, or a wide well containing one barrier off-center from the middle of the well, has been examined in order to understand tunneling processes. A possible explanation is based on the fact that the different quasibound states of such a structure react differently to an applied bias voltage and to changes in the widths and depths of the wells. There are two interpretations of the tunneling process, one that electron tunneling is phonon assisted, and the other that impurity tunneling dominates over phonon-assisted tunneling. These two explanations are described briefly below.

Oberli and coworkers²⁻⁵ have carried out experimental photoluminescence studies of such an asymmetric structure mentioned above where one narrow well (NW) and one wide well (WW) are coupled through a wide barrier. The properties of this structure, such as tunneling time, were explored, and it was found that under a bias, the quasibound states of the system coincide for a certain strength of the applied voltage, giving rise to resonant tunneling of carriers. In other words, their studies showed a minimum in the decay time versus applied voltage at the resonance. It is obvious that the decay time will be shorter when two states are aligned. Experiments were performed for two samples, one with NW and WW and the other with WW and NW. The interchange of NW and WW is important since changes brought about to the quasibound states by the applied field are different for two different combinations. In the first case, NW and WW, the respective widths were 60 and 88 Å. Three different barrier widths of 40, 55 and 65 Å were considered. For the barrier width of 55 Å, resonance between the second and third quasibound states, which are actually the ground state of NW and first-excited state of WW, respectively, occurred at a

strength of 64 kV/cm of the applied field. and the measured transition time was 7.5 ps.² Oberli et al also did a Monte Carlo calculation for the coherent time,⁵ and the calculated time was found to be significantly lower (0.67 ps) than the observed one, though the general pattern was reproduced.

In a second set of observations,^{3,4} the widths of WW and NW were 110 and 70 Å, respectively. A minimum was found at 48 kV/cm in the variation of decay time as a function of applied voltage. At this voltage the difference between the ground states of NW and WW is equal to the optical phonon energy, which is a signature of phonon-assisted tunneling. We should note here that *AlGaAs* exhibits a two-mode behavior, such that the scattering of a longitudinal optical phonon occurs at two distinct energies, approximately 35 and 47 meV, for 35% aluminum fraction.

A similar study was also done for a structure similar to the one above by Liu et al⁶ and Deveaud et al⁷. In these two works, the resonance condition was met either by an applied electric field or by changing the width of the one of the wells. In principle, the changes brought about by an electric field, which essentially alters the depths of the wells or their widths, are the same. This can be demonstrated by introducing a dimensionless parameter $\gamma = \sqrt{\frac{m^*}{\hbar^2}} V d^2$, where V and d are the well depth and width. For a given γ , several combinations of V and d can be found to give the same states of the well. Liu, Deveaud and coworkers^{6,7} concluded that impurity tunneling dominates over optical phonon tunneling.

In this paper we calculate the position expectation value $\langle x \rangle_i$ of an electron in the three consecutive quasibound states of the asymmetric system considered by Oberli and coworkers⁵ as a function of an applied field. Our intention here is not to resolve the discrepancy regarding the tunneling process but merely to demonstrate that for a certain strength of the applied field, the most probable position to find an electron at a state may lie in the barrier separating two wells. As anticipated, $\langle x \rangle_1$, which is the position expectation value of an electron in the ground state of WW, moves towards the left wall of the well as the applied voltage increases, but

the field dependency is very weak. $\langle x \rangle_2$ and $\langle x \rangle_3$, which are the position expectation values of an electron in the ground state of NW and the first-excited state of WW extend inside barrier, and they also seem to interchange their identities.

There have been several investigations aimed at finding a new type of infrared detector fabricated out of semiconductor heterostructures and operating on the principle of intersubband or interband transitions.⁸⁻¹¹ Recently, it was shown that not only are such detectors feasible, but there are ways to tailor their wavelengths to desired values.^{10,11} One of the tailoring^{10,11} methods is based on the symmetric and antisymmetric properties of the subbands of the well. These model investigations include one extra layer in the middle of the well or a delta function potential located in the neighborhood of the middle of the well, so that the antisymmetric states stay practically unchanged, whereas the change in the symmetric states will change the transitions frequencies.

As we shall see in this paper, a similar tailoring is also possible for the asymmetric structures mentioned above. In this case, an electric field lowers the ground state and first-excited state of WW up to the resonance voltage, whereas the oscillator strength for the transition between them hardly changes. For an applied voltage greater than the resonance value the oscillator strength drops to almost zero, whereas the energy difference between these two states increases as the applied voltage increases. Our aim in this paper is not to study infrared detectors but to demonstrate the interchange of identities between the second and third quibound states of the whole structure utilizing the oscillator strength, and also resonant tunneling between these two states.

We shall see below (Sec. 3) that the transition probability, i.e., oscillator strength, from the first to the second state of the system is very small up to the resonance voltage, which is unlikely so far as the selection rules are concerned. It seems that the asymmetric location of the barrier alters the symmetry of the states. But as mentioned earlier, a small oscillator strength is not surprising since this transition is between the ground states of WW and NW. For an applied voltage greater than the resonance voltage, the ground state of NW and

first-excited state of WW interchange their identities, making a transition probable. A similar observation is also found for the oscillator strength for the transition from the first to the third state of the system. The oscillator strength for the transition from the second to third state of the system remains practically zero, implying that the transition between these two states is not probable except in the neighborhood of the resonance voltage where it peaks. This oscillator strength variation with applied voltage has been fitted to a Lorentzian distribution, and it is found that the width of the resonance tunneling depends strongly on the width of the barrier separating the two wells.

2. Method of Calculation

The Schrödinger equation for the potential profile such as the one discussed earlier, a square well with a field linearly varying with the position, has been solved applying the boundary conditions. A brief formalism to calculate the eigenvalues and eigenfunctions of an asymmetric double quantum well under bias based on the matrix method is described in the Appendix. Let us suppose that ϵ_i and $\Psi_i(x)$ are the eigenvalue and eigenfunction of the state i . Then $\langle x \rangle_i$ can be calculated as

$$\langle x \rangle_i = \int_{-\infty}^{\infty} \Psi_i^2(x) x dx, \quad (1)$$

and the oscillator strength f_{ij} for the transition from state i to state j by the expression

$$f_{ij} = \frac{2m_0}{\hbar} \omega |M_{ji}|^2, \quad (2)$$

where m_0 is mass of the electron, $\omega = \frac{\epsilon_j - \epsilon_i}{\hbar}$ is the frequency of the transition and M_{ji} is the dipole matrix element. is given by

$$M_{ji} = \int_{-\infty}^{\infty} \Psi_j(x) x \Psi_i(x) dx.$$

3. Results and Discussions

An asymmetric double quantum well with widths 60 and 88 Å separated by a barrier under bias is now analyzed. Three different barrier widths of 40, 55 and

65 Å are considered. The well depths are given by the formula¹² $V_0 = 0.65(1155y + 37y^2)$, where V_0 is in meV, and y is the fraction of Al in the AlGaAs layers forming the barrier and the walls. Utilizing the procedure described in the Appendix, the eigenvalue and eigenfunction of the first three quasibound states of the system are calculated, and then $\langle x \rangle_n$ and f_{ij} are determined using Eqns. (1) and (2).

In Fig. 1 we show the position expectation value $\langle x \rangle_1$ of the first quasibound state, for three different barrier widths as a function of the applied field. The solid, dashed and dot-dashed lines correspond to barrier widths of 40, 55 and 65 Å. The unbiased structure with a 55 Å barrier is also shown by the solid line to guide the eye of the reader to the most probable location of the electron in the state. A scaling factor has been used to show the structure. As mentioned earlier, the location of this state lies in WW. The changes brought about by the field are very small. A linear fit to the shift in position, $\langle x \rangle_1^F = \langle x \rangle_1^0 + \delta F$, yields the values of $\delta = 9.8, 9.6$ and $9.5 \text{ Å}^2/\text{mV}$ for barrier thicknesses of 40, 55 and 65 Å, respectively. The shift in position towards the right wall of the structure is greater for the thinner barrier than for the thicker barrier because the wells are more loosely coupled in the latter case.

Figures 2 and 3 show the changes in position expectation values of the second and third quasibound states of whole structure. $\langle x \rangle_2$ and $\langle x \rangle_3$, as the applied field increases. Again, it is clear that the second quasibound state is the ground state of NW (Fig. 2), and the third is the first-excited state of WW (Fig. 3) up to a certain applied voltage, namely the resonance voltage. Above this resonance voltage, these two states exchange their identities, meaning that the second and third quasibound states are now the first-excited state of WW and the ground state of NW, respectively. More discussion about the interchange of identities is given below. For demonstration purposes, a scaled structure with a 55 Å barrier and no bias is also shown in Figs. 2 and 3.

It is further clear from Figs. 2 and 3 that in the vicinity of the resonance voltage, the most probable position to find an electron is within the barrier separating two wells, which in principle is a prohibited region. This means that at resonance there is essentially no barrier

separating the two wells. The transition voltage range, i.e., the range of applied voltage in which there is a finite probability to find an electron within the barrier, is found to be a function of the barrier width. A quantitative description of this is given below.

The results of the oscillator strength for transitions from the first quasibound to the second and third quasibound states are shown in Figs. 4 and 5. The oscillator strength for the transition from the first to the second quasibound state (see Fig. 4) remains practically zero up to the resonance voltage. The reason is that this transition is from the ground state of WW to the ground state of NW, which is prohibited by selection rules. Within the transition voltage range, the oscillator strength reaches a constant value, implying that the transition from the first to the second quasibound state is probable. This is possible only if the symmetry of the second quasibound state has been altered. It has been noted earlier that the identities of these two states get interchanged above the resonance voltage, i.e., in the transition voltage range, which is another way of looking at the interchange of identities.

In Fig. 5 the oscillator strength for the transition from the first to the second quasibound state, which is the transition from the ground to the first-excited state of WW, decreases very slowly as the applied voltage increases up to the resonance value and goes to almost zero for the applied voltage greater than this value. Once again, it is found that the identities of the second and third quasibound states interchange. It is worth noting here that at voltages less than the resonance voltage, the oscillator strength for the transition from the first to the second states increases considerably slower than the decrease in the oscillator strength for the transition from the first to the third. In other words, $\left| \frac{df_{ij}(1-3)}{dF} \right| > \left| \frac{df_{ij}(1-2)}{dF} \right|$ for voltages less than the resonance value.

Figure 6 shows the oscillator strength for the transition from the second to the third quasibound state, which are actually the ground state of NW and first-excited state of WW. Per the usual rule, this transition is most probable but this does not appear so from Fig. 6. The oscillator strength remains almost zero except in the range of transition voltage where it forms a peak. It

is quite obvious that a peak in oscillator strength versus applied voltage occurs at the resonance voltage, meaning that this transition is only allowed when these two states are aligned. This resonance condition is met at a lower applied voltage when the thicker barrier is separating the two wells, and the maximum value of oscillator strength is reduced. The width of this resonance, which may be called the transition voltage, gets sharper as the barrier thickness increases. As this increase occurs, the two wells become loosely coupled, and there is a thickness for which transitions between these two states are negligible since the electrons can no longer tunnel through the barrier.

Since the peak in the oscillator strength versus applied voltage is the result of resonance tunneling of the carrier from one well to the other through a barrier, this distribution can be characterized by a Lorentzian distribution. We have fitted the oscillator strength to a Lorentzian distribution.

$$f_{ij}(2 \rightarrow 3) = \frac{C}{1 + (F - F_R)^2 / \Gamma^2}, \quad (3)$$

where F_R is the resonance voltage, Γ is the half width at full maximum (HWF) and C is a constant and function of the maximum value of the oscillator strength and Γ . The transition voltage can be taken to be twice Γ . Fitted and inferred from Fig. 6, the values of Γ and F_R are plotted in Fig. 7 as function of the barrier width. The resonance voltages for different barrier thicknesses are in agreement with the fitted values, whereas the HWF are about 20% smaller than the fitted ones.

4. Conclusions

In summary, we have performed calculations for the position expectation values of an electron in different quasibound states of an asymmetric double quantum well under bias and found that the first three quasibound states of the structure are actually the ground state of WW, the ground state of NW and first-excited state of WW. The ground state of NW and the first-excited state of WW get aligned at a certain applied voltage called the resonance voltage, and above this resonance voltage these two states interchange their identities. The probability to find an electron in one of these

states in the transition voltage range, i.e., the range of the applied field in which these two state interchange their identities. lies within the barrier, which implies that at resonance a barrier does not exist for these two states.

We have also done a calculation for the oscillator strength for transitions from the first to the second and third quasibound state, and from the second to the third. Interchange of the identities between the second and third quasibound states is confirmed. The oscillator strength of the transition from the second to the third quasibound state peaks at the resonance voltage. A fit of oscillator strength versus applied voltage to a Lorentzian distribution yields very good agreement with the calculated values. This is the signature of resonance tunneling from the second to the third state through the barrier.

Acknowledgements- This research was supported by the Office of Naval Research. Part of the calculation was done utilizing the facilities at the Pittsburgh Supercomputing Center under Grant No. PHY890020P.

Appendix

A general Schrödinger equation for any of the regions including the structure under bias can be written as

$$\frac{d^2\psi(x)}{dx^2} + \frac{2m^*}{\hbar^2}[E - V(x) \pm eFx]\psi(x) = 0, \quad (A1)$$

where

$$V(x) = \begin{cases} V_0, & \text{if } x \leq x_1, x_2 \leq x \leq x_3 \text{ and } x \geq x_4, \\ 0, & \text{otherwise.} \end{cases}$$

Here, F is the external applied electric field (normally measured in voltage per unit length), and m^* is the effective mass taken differently in different regions depending upon the fraction of Al in the layer. The value of the effective mass has been determined by the expression¹² $m^* = 0.067 + 0.088y$, where y is the fraction of Al in $AlGaAs$. The \pm sign refers to the forward and backward bias. The points x_1 to x_4 are the boundaries at which the wavefunctions and their derivatives divided by the effective mass of the regions should be continuous, and are defined for the present case as

$$x_1 = -(d_n + d_w + d_b)/2,$$

$$x_2 = (d_n - d_w - d_b)/2,$$

$$x_3 = (d_n + d_b - d_w)/2,$$

$$x_4 = (d_n + d_w + d_b)/2,$$

where d_n , d_b and d_w are the widths of NW, barrier and WW, respectively. The energy and position x are measured from the middle of the structure.

By a simple coordinate transformation, Eq. (A1) can be written as

$$\frac{d^2\psi[\rho(x)]}{d\rho^2} - \rho(x)\psi[\rho(x)] = 0, \quad (A2)$$

whose solutions are the Airy function $Ai[\rho(x)]$ and its complement $Bi[\rho(x)]$. Here $\rho(x)$ is the new coordinate system and related with x as

$$\rho(x) = \alpha(m^*)[\mp x + \frac{V_0 - E}{eF}],$$

with $\alpha(m^*) = [2m^*/eF\hbar^2]^{1/3}$. Hence, the wavefunction in the different regions can be given as

$$\psi_i(x) = a_i Ai[\rho(x)] + b_i Bi[\rho(x)] , \quad (A3)$$

where a_i and b_i are the wavefunction amplitudes, and the subscript i ranges from the region to the left of x_1 to the region to the right of x_4 . These amplitudes a_i and b_i can be calculated by applying the boundary conditions, whereby the wavefunction and its derivatives divided by the effective mass of the region should be continuous across the interface.

Following the matrix method, the amplitudes a_5 and b_5 in the region to the right of x_4 can be expressed in terms of a_1 and b_1 in the region to the left of x_1 as

$$\begin{bmatrix} a_5 \\ b_5 \end{bmatrix} = M \begin{bmatrix} a_1 \\ b_1 \end{bmatrix} , \quad (A4)$$

where M is a 2×2 matrix resulting from the boundary conditions and given as

$$M = M_{x_4}^{-1}(R) M_{x_4}(L) M_{x_3}^{-1}(R) M_{x_3}(L) M_{x_2}^{-1}(R) M_{x_2}(L) M_{x_1}^{-1}(R) M_{x_1}(L) . \quad (A5)$$

The subscripts on the matrices indicate the interface where two regions meet, and L and R stand for the left and right of the interface. For example, the matrix of the region to the left of the interface x_4 for forward bias can be given as

$$M_{x_4}(L) = \begin{pmatrix} Ai(\beta) & Bi(\beta) \\ \frac{-\alpha}{m_4^*} Ai'(\beta) & \frac{-\alpha}{m_4^*} Bi'(\beta) \end{pmatrix} .$$

Here, $\beta = -\alpha(m_4^*)[x_4 + \frac{E}{eF}]$, $Ai'(\beta) = \frac{dAi(\rho)}{d\rho} |_{\rho=\beta}$ and m_4^* is the effective mass of the electron in the region to the left of x_4 . The Wronskian $Ai(\alpha)Bi'(\alpha) - Ai'(\alpha)Bi(\alpha) = \frac{1}{\pi}$ of Airy functions can be very useful to find the inverse of the matrices. In the case of a forward bias, for the wavefunction to be bound, the amplitude b_1 should be zero, because as x decrease in the first region, $Bi[\rho(x)]$ increases monotonically and tends to ∞ . In region 5, the amplitude a_5 should be zero, giving rise to the following condition for quasibound states of the system:

$$a_5 = M(1, 1)a_1 = 0 . \quad (A6)$$

For all the practical purposes, α_1 can be taken to be unity, although it can be found from the normalization condition, $\int_{-\infty}^{\infty} |\psi(x)|^2 dx = 1$.

The quasibound states of the system can be found by finding the zeroes of the function $f(E) = M(1, 1)$ by varying E . An analytic expression of $f(E)$ can be given in terms of the Airy and complementary Airy functions calculated at the interfaces, but it is very lengthy and is omitted here for the purpose of brevity. However, a numerical solution of $f(E) = M(1, 1)$ can be found easily and accurately. Once the eigenvalue is determined, one can calculate M for the energy equal to the eigenvalue, and the amplitude of the wavefunction in the region to the right of x_4 can be calculated by $b_5 = M(1, 2)$. The amplitudes of the wave function in the remaining regions then follow from the matrix method.

References

1. L. Esaki and R. Tsu, Appl. Phys. Lett. 22, 562 (1970); IBM J. Res. Dev. 14, 61 (1970).
2. D.Y. Oberli, J. Shah, T.C. Damen, C.W. Tu, T.Y. Chang, D.A.B. Miller, J.E. Henry, R.F. Kopf, N. Sauer and A.E. DiGiovanni, Phys. Rev. B 40, 3028 (1989).
3. D.Y. Oberli, J. Shah, T.C. Damen, J.M.Kuo, J.E. Henry, J. Lary and S.M. Goodnick, Appl. Phys. Lett. 56, 1239 (1990).
4. D.Y. Oberli, J. Shah, T.C. Damen, J.M. Kuo, R.F. Kopf and J.E. Henry, Surf. Sci. 229, 189 (1990).
5. J. Lary, S.M. Goodnick, P. Lugli, D.Y. Oberli and J. Shah, Solid-State Electronics 32, 1283 (1989).
6. H.W. Liu, R. Ferreira, G. Bastard, C. Delalande, J.F. Palmier and B. Etienne, Appl. Phys. Lett. 54, 2082 (1989).
7. B. Deveaud, F. Clerot, A. Chomette, A. Regreny, R. Ferreira, G. Bastard, and B. Sermage, Europhys. Lett. 11, 367 (1990).
8. L.C. West and S.J. Eglash, Appl. Phys. Lett. 46, 1156 (1985).
9. B.F. Levine, R.J. Malik, J. Walker, K.K. Choi, C.G. Bethea, D.A. Kleinman and J.M. Vendenberg, Appl. Phys. Lett. 50, 273 (1987).
10. W. Trzeciakowski and B.D. McCombe, Appl. Phys. Lett. 55, 891 (1989).
11. L. N. Pandey, T. F. George and M. L. Rustgi, J. Appl. Phys. 68, 1933 (1990).
12. H.J. Lee, L.Y. Juravel, J.C. Woolley and A.J.S. Thorpe, Phys. Rev. B 21, 659 (1980).

Figure Captions

Fig. 1: Position expectation value for the first quasi-bound state as a function of applied voltage. The structure under analysis is also shown with a scaling factor and barrier width of 55 Å. The scaling factor used to show the structure is $45 + 4V_0/35$. The solid, dashed and dot-dashed lines are for barrier widths of 40, 55 and 65 Å, respectively. The ordinates of this and the following two figures are interchanged just for the convenience of looking at the structure.

Fig. 2: Same as in Fig. 1 but for the second quasibound state.

Fig. 3: Same as in Fig. 1 but for the third quasibound state.

Fig. 4: Oscillator strength as a function of applied field for the transition from the first to the second quasi-bound state. The solid, dashed and dot-dashed lines are for barrier widths of 40, 55 and 65 Å, respectively.

Fig. 5: Same as in Fig. 4, but for the transition from the first to the third quasibound state.

Fig. 6: Same as in Fig. 4. but for the transition from the second to the third quasibound state.

Fig. 7: Half width at full maximum in the upper panel and the resonance voltage in the lower panel as a function of the width of the barrier separating the two wells. The solid circles are the fitted results, whereas the solid triangles are the calculated ones.

Fig. 1

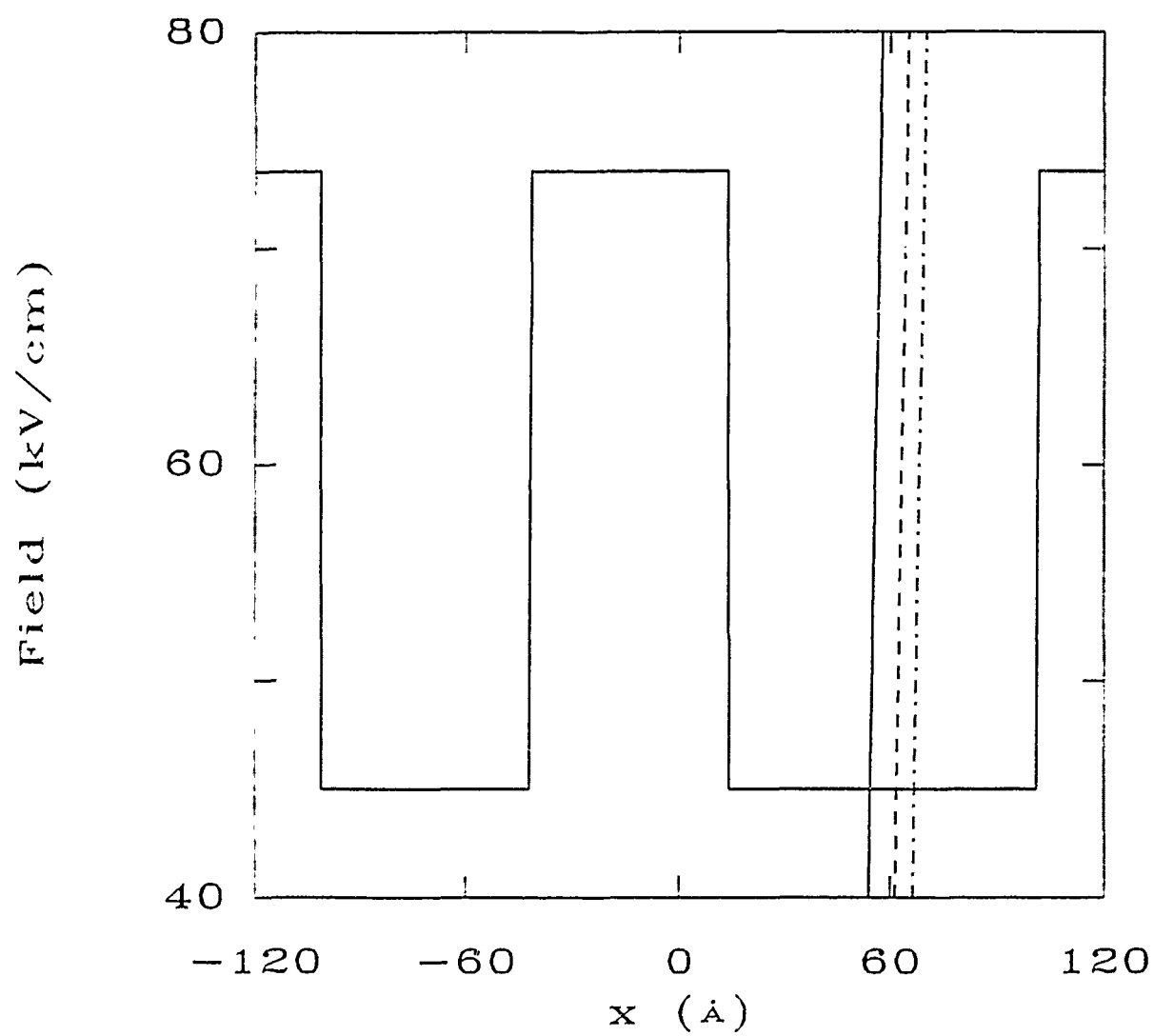


Fig. 2

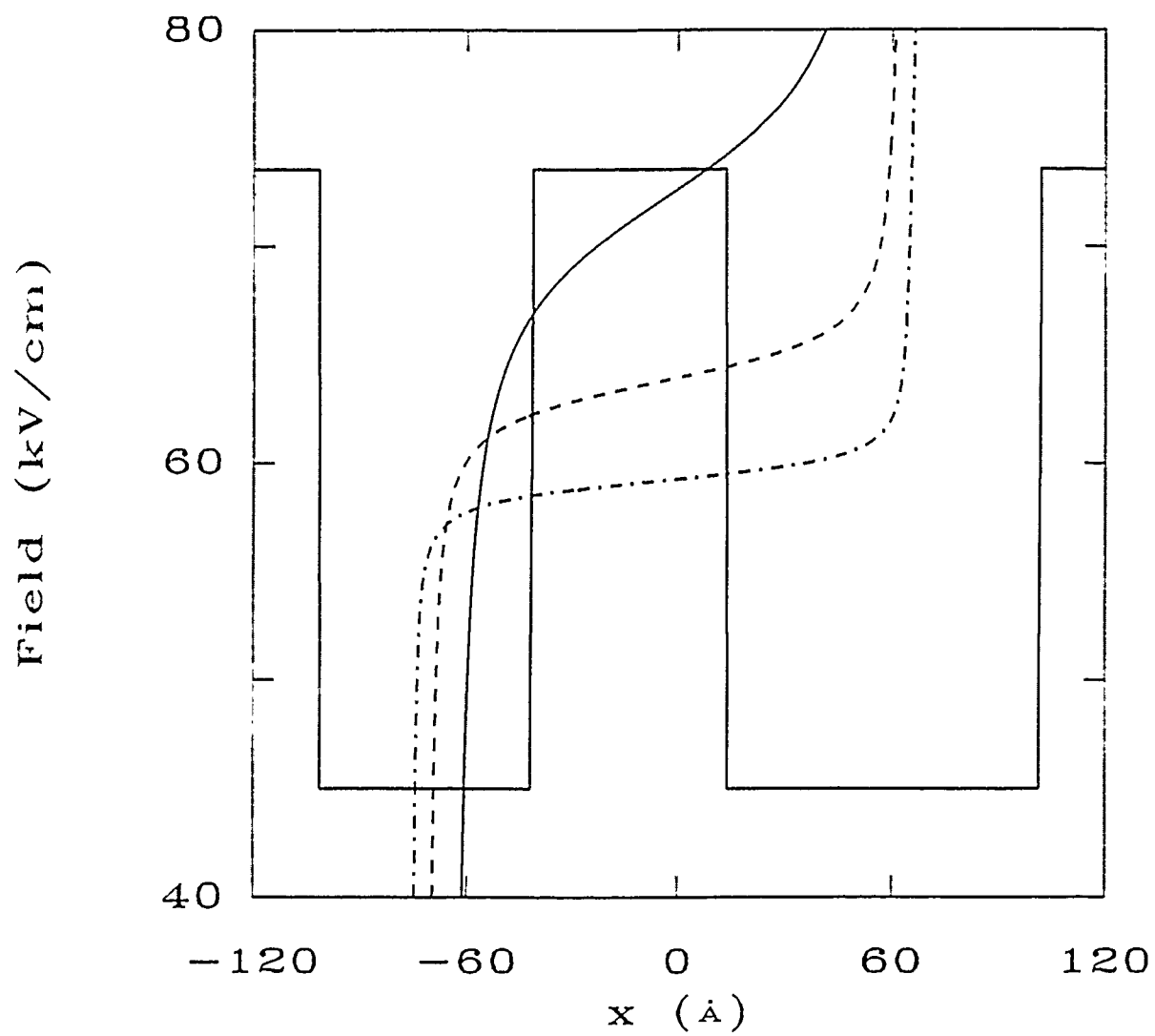


Fig. 3

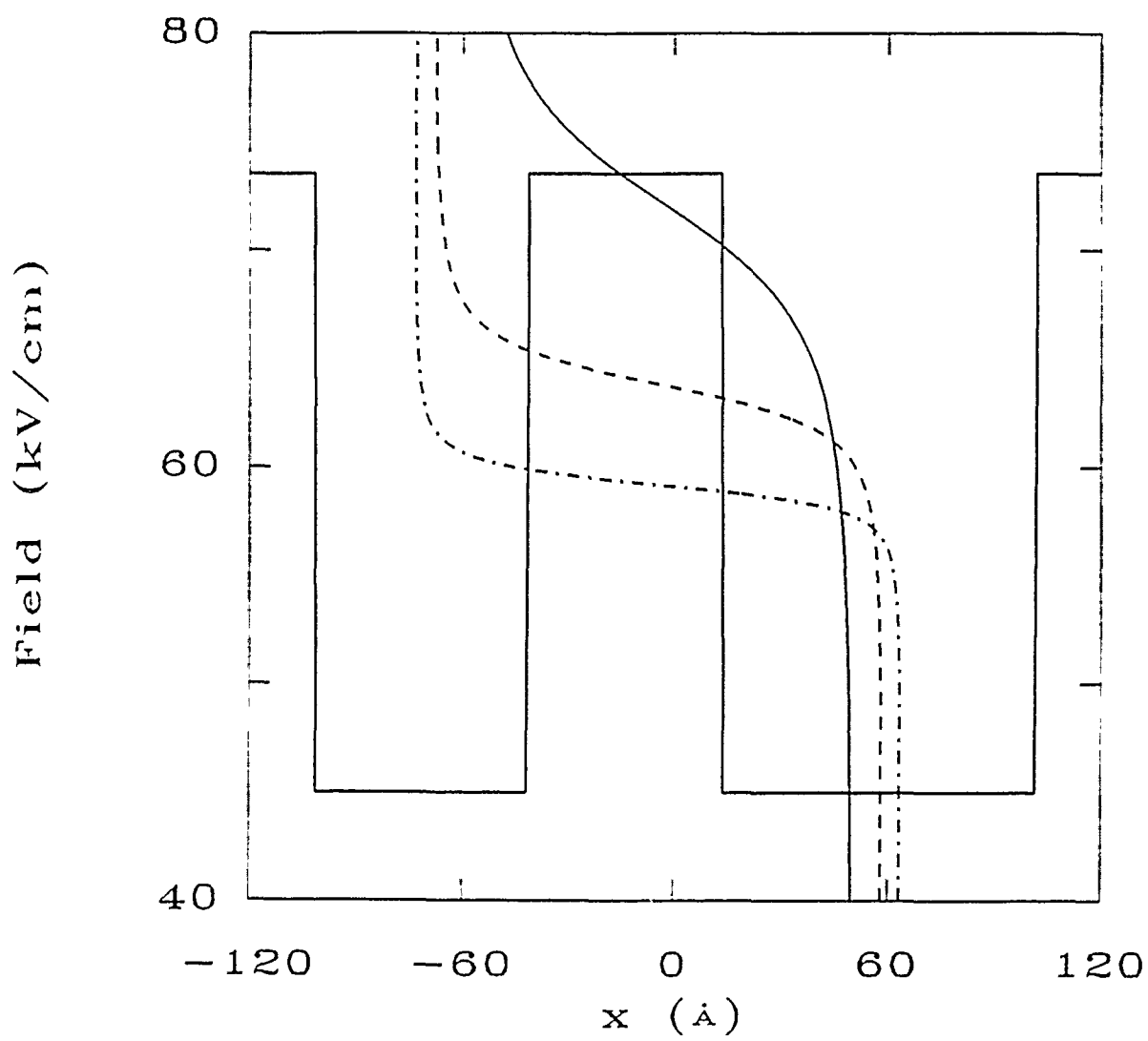


Fig. 4

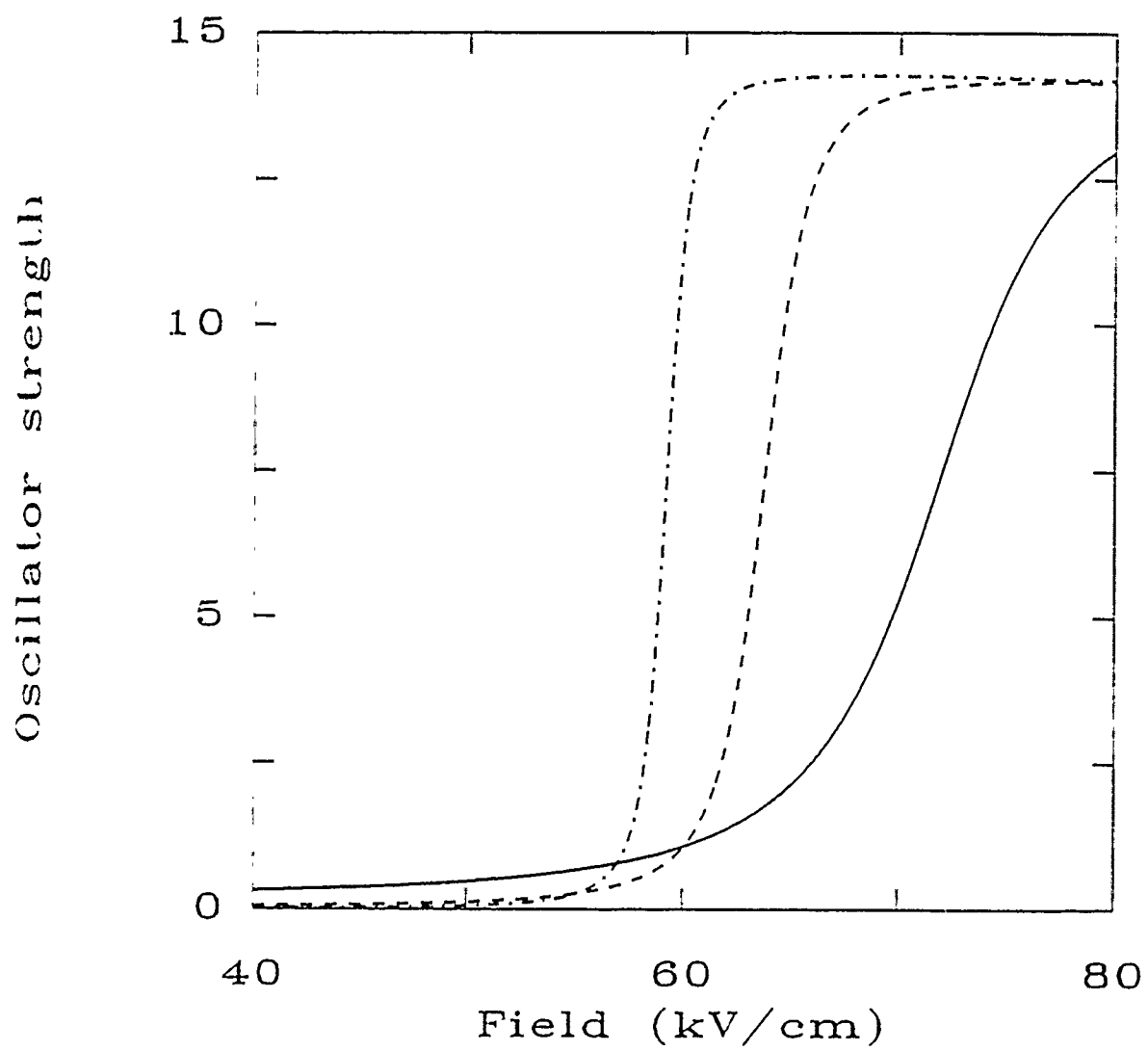


Fig. 5

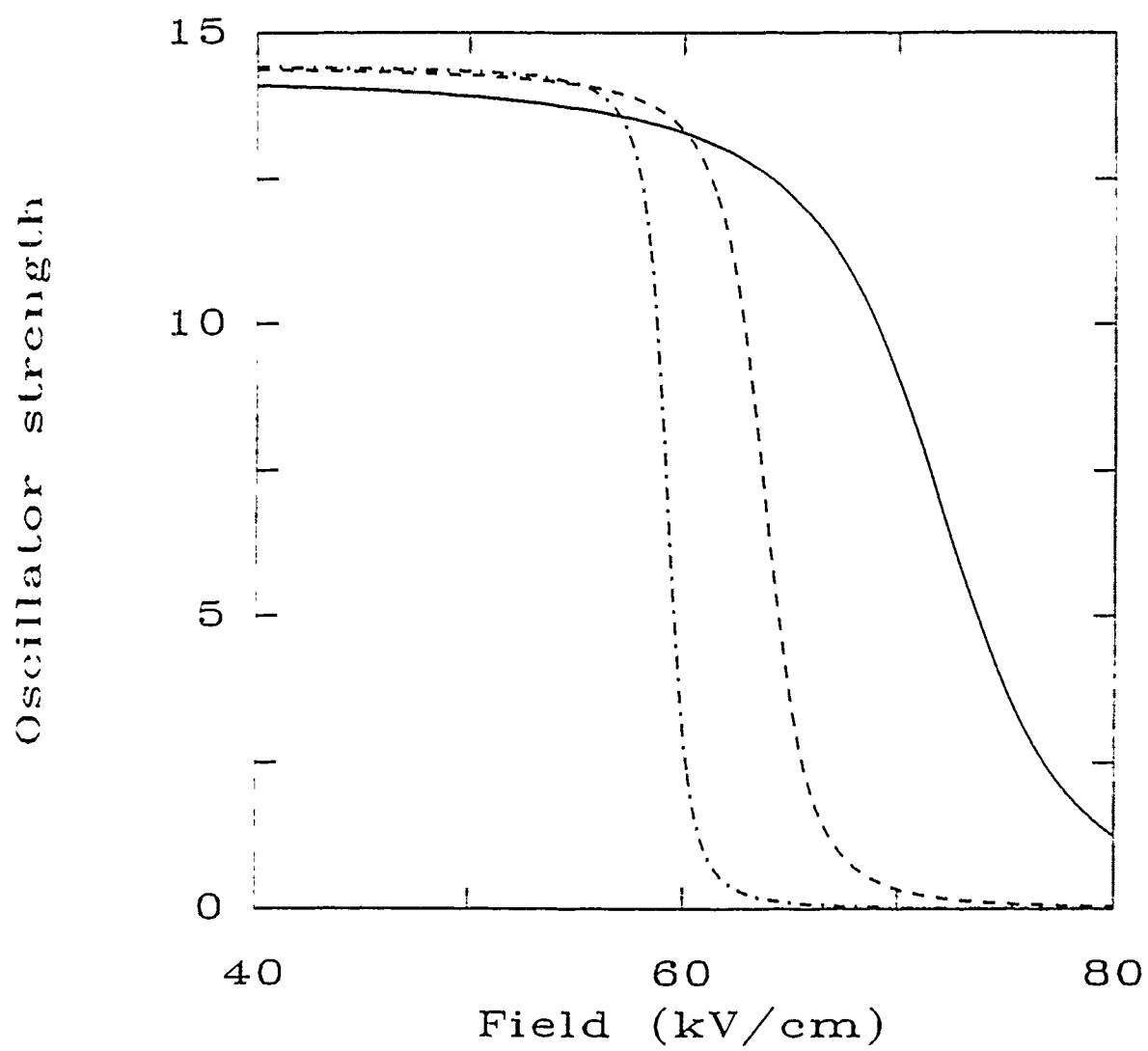
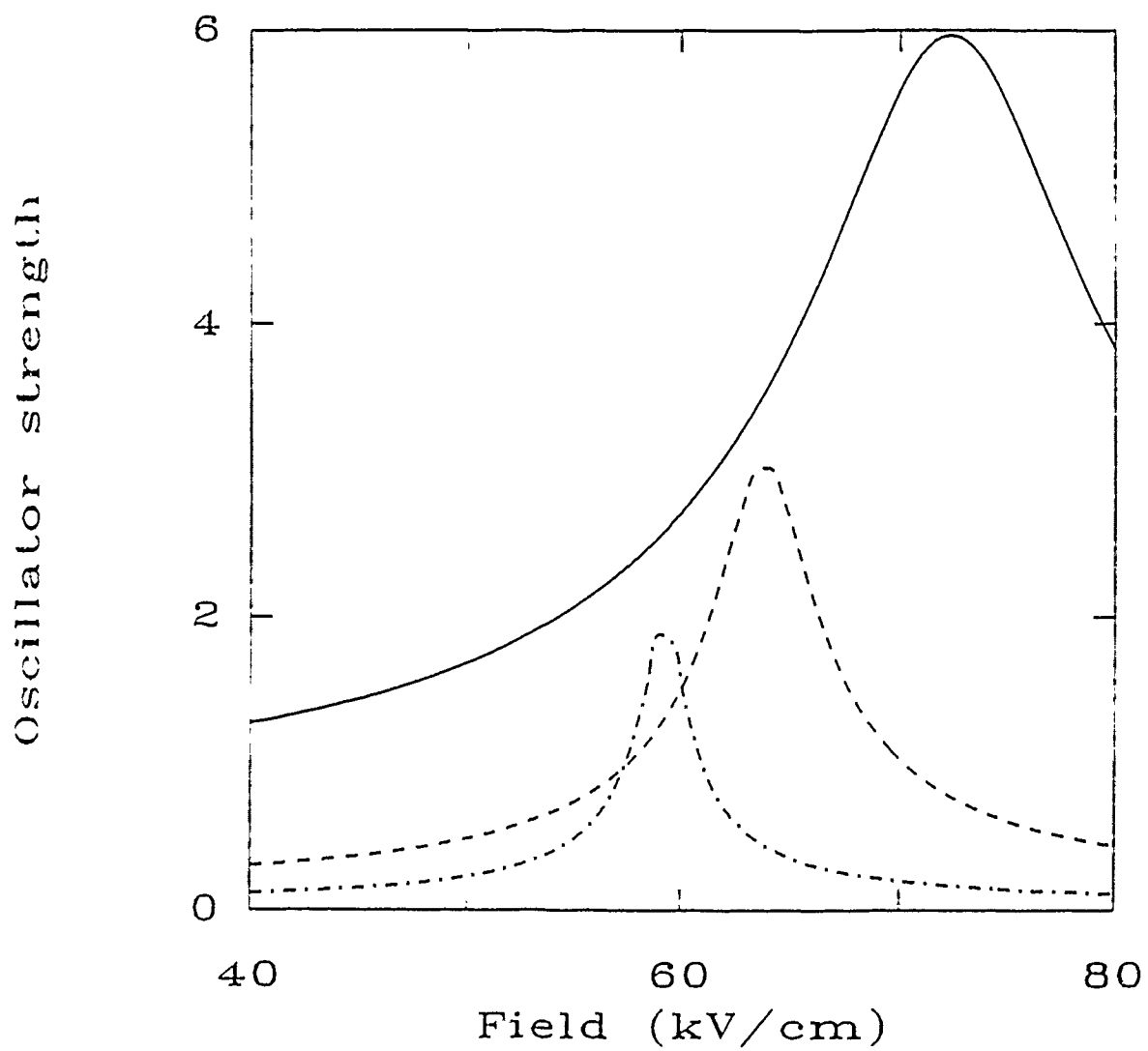


Fig. 6



FY90 Abstracts Distribution List for Solid State & Surface Chemistry

Professor John Baldeschwieler
Department of Chemistry
California Inst. of Technology
Pasadena, CA 91125

Professor John Eyler
Department of Chemistry
University of Florida
Gainesville, FL 32611

Dr. Sylvia Johnson
SRI International
333 Ravenswood Avenue
Menlo Park, CA 94025

Professor Paul Barbara
Department of Chemistry
University of Minnesota
Minneapolis, MN 55455-0431

Professor James Garvey
Department of Chemistry
State University of New York
Buffalo, NY 14214

Dr. Zakya Kafafi
Code 6551
Naval Research Laboratory
Washington, DC 20375-5000

Dr. Duncan Brown
Advanced Technology Materials
520-D Danury Rd.
New Milford, CT 06776

Professor Steven George
Department of Chemistry
Stanford University
Stanford, CA 94305

Professor Larry Kesmodel
Department of Physics
Indiana University
Bloomington, IN 47403

Professor Stanley Bruckenstein
Department of Chemistry
State University of New York
Buffalo, NY 14214

Professor Tom George
Dept. of Chemistry and Physics
State University of New York
Buffalo, NY 14260

Professor Max Lagally
Dept. Metal. & Min. Engineerin.
University of Wisconsin
Madison, WI 53706

Professor Carolyn Cassady
Department of Chemistry
Miami University
Oxford, OH 45056

Dr. Robert Hamers
IBM T.J. Watson Research Center
P.O. Box 218
Yorktown Heights, N Y 10598

Dr. Stephen Lieberman
Code 522
Naval Ocean Systems Center
San Diego, CA 92152

Professor R.P.H. Chang
Dept. Matls. Sci. & Engineering
Northwestern University
Evanston, IL 60208

Professor Charles Harris
Department of Chemistry
University of California
Berkeley, CA 94720

Professor M.C. Lin
Department of Chemistry
Emory University
Atlanta, GA 30322

Professor Frank DiSalvo
Department of Chemistry
Cornell University
Ithaca, NY 14853

Professor John Hemminger
Department of Chemistry
University of California
Irvine, CA 92717

Professor Fred McLafferty
Department of Chemistry
Cornell University
Ithaca, NY 14853-1301

Dr. James Duncan
Federal Systems Division
Eastman Kodak Company
Rochester, NY 14650-2156

Professor Leonard Interrante
Department of Chemistry
Rensselaer Polytechnic Institute
Troy, NY 12181

Professor Horia Metiu
Department of Chemistry
University of California
Santa Barbara, CA 93106

Professor Arthur Ellis
Department of Chemistry
University of Wisconsin
Madison, WI 53706

Professor Roald Hoffmann
Department of Chemistry
Cornell University
Ithaca, NY 14853

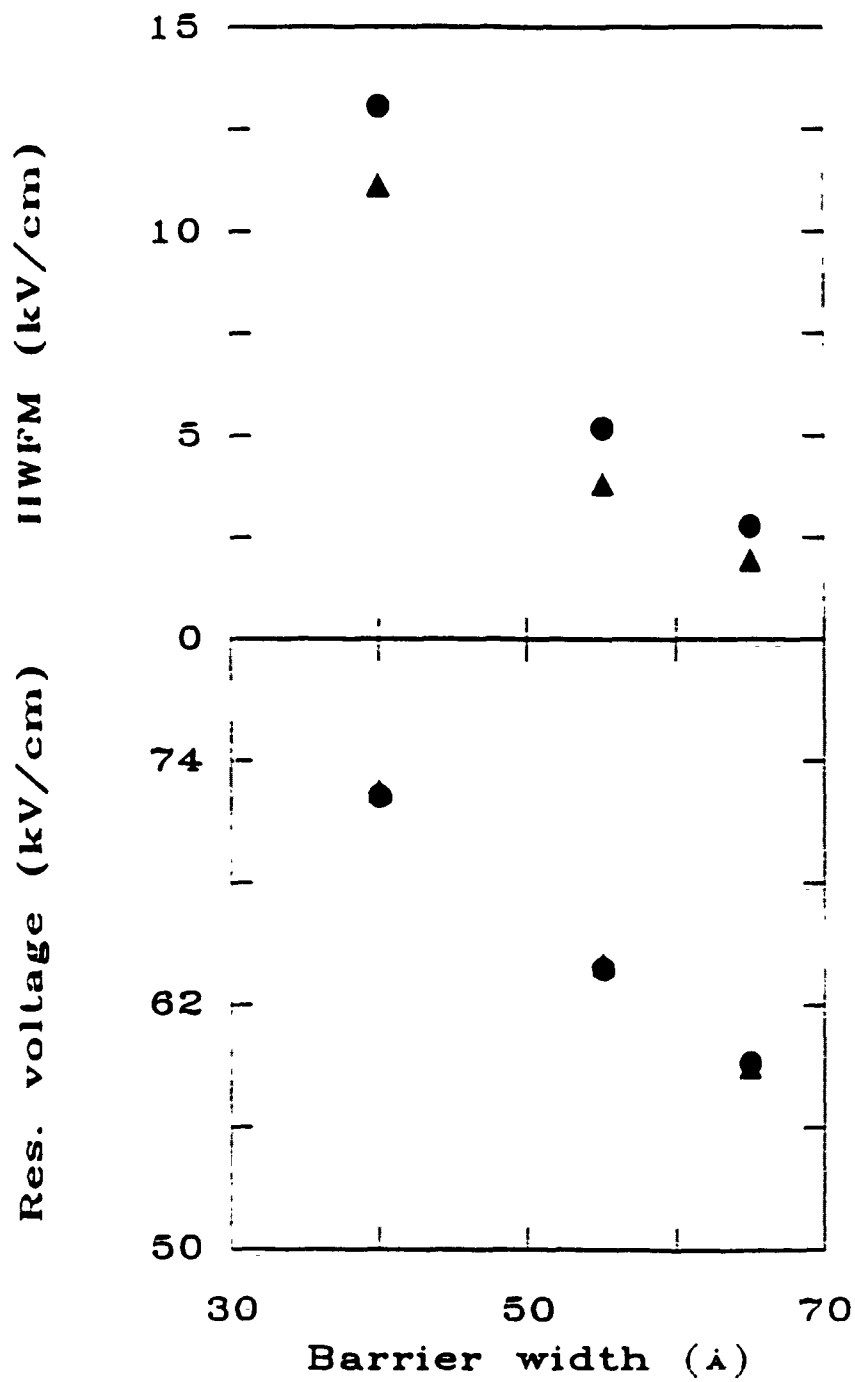
Professor Larry Miller
Department of Chemistry
University of Minnesota
Minneapolis, MN 55455-0431

Professor Mustafa El-Sayed
Department of Chemistry
University of California
Los Angeles, CA 90024

Professor Eugene Irene
Department of Chemistry
University of North Carolina
Chapel Hill, NC 27514

Professor George Morrison
Department of Chemistry
Cornell University
Ithaca, NY 14853

Fig. 7



Professor Daniel Neumark
Department of Chemistry
University of California
Berkeley, CA 94720

Professor Robert Whetten
Department of Chemistry
University of California
Los Angeles, CA 90024

Professor David Ramaker
Department of Chemistry
George Washington University
Washington, DC 20052

Professor R. Stanley Williams
Department of Chemistry
University of California
Los Angeles, CA 90024

Dr. Gary Rubloff
IBM T.J. Watson Research Center
P.O. Box 218
Yorktown Heights, NY 10598

Professor Nicholas Winograd
Department of Chemistry
Pennsylvania State University
University Park, PA 16902

Professor Richard Smalley
Department of Chemistry
Rice University
P.O. Box 1892
Houston, TX 77251

Professor Aaron Wold
Department of Chemistry
Brown University
Providence, RI 02912

Professor Gerald Stringfellow
Dept. of Matls. Sci.
& Engineering
University of Utah
Salt Lake City, UT 84111

Professor Vicki Wysocki
Department of Chemistry
Virginia Commonwealth University
Richmond, VA 23284-2006

Professor Galen Stucky
Department of Chemistry
University of California
Santa Barbara, CA 93106

Professor John Yates
Department of Chemistry
University of Pittsburgh
Pittsburg, PA 15260

Professor H. Tachikawa
Department of Chemistry
Jackson State University
Jackson, MI 39217-0510

Professor William Unertl
Lab. for Surface Sci.
& Technology
University of Maine
Orono, ME 04469

Dr. Terrell Vanderah
Code 3854
Naval Weapons Center
China Lake, CA 93555

Professor John Weaver
Dept. of Chem. Eng. & Mat. Sci.
University of Minnesota
Minneapolis, MN 55455

Professor Brad Weiner
Department of Chemistry
University of Puerto Rico
Rio Piedras, Puerto Rico 00931